Supporting Information

Vaïtilingom et al. 10.1073/pnas.1205743110

SI Text

Cloud Water Collection. Cloud water was sampled from the top of the puy de Dôme mountain (1,465 m above sea level, 45°46′ North, 2° 57′ East, France), as described on the Web site: http://wwwobs.univ-bpclermont.fr/SO/beam. The study location is frequently covered by clouds and is disconnected from local pollution. Two cloud water samplers, developed by Kruisz et al. (1), were used with an estimated cutoff diameter of 7 μm, for an approximately debit rate of 80 $m^3 \cdot h^{-1}$ (2, 3). The collection mechanisms on the cloud water samplers were sterilized using an autoclave (20 min at 121 °C) before sampling, and the body parts were sterilized on site by washing them with ethanol [70% (vol/vol)] and extensively rinsing them with sterile, ultrapure water. After 30 min, to assess the microbial sterility and chemical purity of the freshly cleaned body parts, 50 mL of sterilized, ultrapure water were poured into the sampler and recovered in the collection parts ("blank" samples). For the three cloud-sampling events presented in this article, no microbial or chemical contamination was observed in the "blank" samples.

During sampling, the cloud water was recovered from the collector under sterile conditions when the volume in each collector reached 100 mL. A minimum volume of 600 mL of cloud water was necessary for the biological and chemical analyses listed in Table 1. After collection, samples were immediately frozen or kept at 4 °C. Laboratory experiments were performed less than 2 h after the end of sampling.

Cloud Water Incubation. Half of the sample was sterilized by filtration (filter porosity 0.22 μm, nylon filter) to eliminate microorganisms. The filtered and unfiltered samples were incubated for 7 d in the dark or under UV light. The experiments were carried out at a constant temperature of 17 °C, a value slightly different from the temperature during the cloud-sampling events (10 °C, 13.5 °C, and 10 °C, for clouds 1, 2, and 3, respectively). The incubator chamber was equipped with a stirring plate (aerobic condition, 110 rpm) under a fluorescent tube that emitted radiation with wavelengths between 340 and 420 nm (λ_{max} = 365 nm and total light energy: 33 $J \cdot s^{-1} \cdot m^{-2}$). For incubation in darkness, two brown 250-mL Erlenmeyer flasks were used. For incubation under UV light emission, two photo-bioreactors were used (Fig. S1). These photo-bioreactors consisted of a cylindrical Pyrex crystallizer (300 mL, 95-mm diameter) covered with a Pyrex glass filter (3.3-mm thick and 80 mm Ø) and mounted on a nylon lid that was equipped with eight vents (Teflon tubes of 8 mm Ø, plugged with sterile cotton wool to avoid microbial contamination) to prevent water condensation on the filter and to maintain continuous oxygenation in the tested medium. Preliminary tests in artificial cloud-water solutions have shown that there was no effect of the incubation flask type on the transformation rates. Biological and chemical analyses were conducted after the cloud water collection and at various times during the incubation, as indicated in Table 1.

Chemical Analyses. ***Conductivity, pH, total and dissolved organic carbon.*** Conductivity and pH were measured on-site with a portable multiparameter pH-meter that was equipped with a temperature sensor. The total organic carbon (TOC) and dissolved organic carbon (DOC) were measured with a TOC analyzer (TOC 5050A, Shimatzu). Five milliliters of filtered (filter porosity 0.22 μm) and nonfiltered samples were used for DOC and TOC measurements, respectively, as described in Parazols et al. (4).

Fe(II), Fe(III). The iron (Fe) concentrations [Fe(II) and Fe(III)] were measured with a spectrophotometric assay with a colorimetric complexant (ferrozine) (5) that was used for cloud water analyses by Parazols et al. (4). To determine the concentrations of Fe(II) and Fe(Total), 2 × 1-mL samples were necessary. The uncertainty in the measurements was less than 10%, and the detection limit (DL) was 0.1 μM (calculated as three times the SD of the field blanks).

Ionic species. The ion concentrations in the cloud water samples were measured using ionic chromatography (3, 6) units: Dionex DX320 for anions (column AS11, eluent KOH) and Dionex ICS1500 for cations (column CS16, eluent hydroxymethanesulfonate acid). Samples were thawed 15 min before their dilution by a factor of 10 in ultrapure water and transferred into vials (5 mL) previously rinsed with ultrapure water. No chemical transformations were observed in our samples after one freeze/thaw cycle. The accuracy of the ion chromatographic analyses was 5% (3).

Formaldehyde. The formaldehyde concentration was measured using a miniaturized fluorimetric assay that was adapted from Li et al. (7). The reaction medium included 60 μL of ammonium acetate solution (4 M), 60 μL of acetoacetanilide [0.2 M in ethanol solution 50% (vol/vol)], 60 μL of ethanol (96°) and 120 μL of the cloud water sample. The solutions were mixed and incubated on a plate with 96 black, flat-bottomed wells at room temperature for 25 min before reading (λ_{ex} = 375 nm and λ_{em} = 490 nm). The uncertainty in the measurements was less than 5%, and the DL was 0.1 μM (calculated as three times the SD of the field blanks).

H_2O_2. The hydrogen peroxide concentration was measured using an accurate enzymatic fluorimetric assay with a 4-Hydroxyphenylacetic acid that produced a fluorescent dimeric compound with hydrogen peroxide [microassay adapted from Lazrus et al. (8)]. Next, 1.5 mL of a solution of 4-Hydroxyphenylacetic acid (1.5 mM) in a phosphate buffering solution (0.1 M, pH 7.4) was mixed with 10 μL of a horse radish peroxydase solution (380 units/mL^{-1}) to constitute the reagent solution; this solution was kept at 5 °C for less than 12 h. After sampling (less than 5 min), 10 and 50 μL of the cloud water sample were mixed on-site with 200 μL of the reagent solution in duplicates and incubated at room temperature (>17 °C) for 5 min before freezing at −25 °C. A new calibration was systematically performed before each analysis session, with a normalized H_2O_2 solution with a different concentration (0–200 μM) using the same reagent lot. Before the analysis, the mixed samples (cloud water + reagent) were thawed at ambient temperature for 10 min, and 200 μL were analyzed. Previous tests indicated that the fluorescent dimeric compound remained stable after this freeze/thaw process. Fluorescence readings (λ_{ex} = 320 nm and λ_{em} = 390 nm) were made in a 96-well format. The uncertainty of the measurements was less than 5%, and the detection limit was 0.07 μM.

To determine the concentration of organic peroxides, samples were treated with catalase. After 30 s, 200 μL of the reagent solution was added, and the previous protocol was applied. For all cloud waters, the organic peroxide concentrations were lower than the limit of detection (0.07 μM).

Biological Analyses. A direct enumeration of cells (duplicates, 10 mL) was performed with epifluorescence microscopy, as described by Amato et al. (9). The main difference in methods was in the use of a phosphate buffering solution (pH = 7) to improve the fluorescence efficiency.

The ATP and ADP concentrations were measured in cloud water samples (0.2 mL) using the ATP Biomass Kit HS (Biothema) and a Biolumineter (Lumac Biocounter M2500). The analytical protocol was described in ref. 10.

The cloud water samples (0.2 mL) were strongly mixed in situ in a sterile microtube with an equal volume of extractant B/S, from the ATP Biomass Kit HS (Biothema). This mixture was used for ATP determination and was stored frozen before the analysis. The ATP concentrations were determined by bioluminescence (11, 12) using a Biolumineter (Lumac Biocounter M2500). The ADP concentration was determined after the direct transformation of ADP to ATP in the luminometer tube, in the presence of pyruvate kinase and phosphoenolpyruvate; this analytical protocol is described in ref. 10. A small volume of the mixture (sample + extractant B/S: 60 μL) was used to determine the ATP or ADP concentration.

Calculations of the Transformation Rates. To calculate the initial transformation rates, the temporal evolution of the concentration of each compound was plotted. Then, the pseudofirst order decay "k" (s^{-1}) was determined (only for $r^2 > 0.8$) using the following linear regression:

$$\ln([C]/[C]_0) = f(t) = -k \times t.$$

The transformation rate of the compound C (v_c) was determined as follows:

$$v_c = k \times [C]_t \quad [M^{-1}\ s^{-1}],$$

where $[C]_t$ is the concentration of the chemical compound C ($mol \cdot L^{-1}$) at time t (s), and k is the pseudofirst order decay (s^{-1}).

H_2O_2 Degradation: Relative Contribution of Biotic and Abiotic Processes. To quantify the relative impact of biotic activity compared with abiotic H_2O_2 transformations, we corrected some of our data. We used the initial degradation rate of H_2O_2 in the absence of microorganisms and light (reference sample) to quantify the impact of the radical reactions that were nonphotochemically induced. For photodegradation and biodegradation, we have subtracted this value from the initial rates that were measured in the presence of light, or microorganisms, respectively (Table S2). From these corrected values, it was possible to calculate the relative contribution of each type of reaction (Fig. S3).

Bio- and Phototransformation of Carboxylic Acids and Formaldehyde in Cloud Samples. The concentrations of formate, acetate, succinate, oxalate, malonate, and formaldehyde were recorded at 17 °C under four incubation conditions ("Microorganisms + Light," "Light," "Microorganisms," and "Reference") for the three cloud water samples (Fig. 3, and Figs. S4 and S5). The transformation rates that were measured in these experiments are listed in Table S3.

Under dark conditions with the endogenous microbial population (Microorganisms case), the acetate and formate biodegradation rates were much higher than those of succinate, malonate, and formaldehyde for the three cloud events. For formate, a lag time was observed in clouds 1 and 2, as already noted for cloud 2. For malonate, two kinetic steps took place in clouds 2 and 3: until 36 h, the rates were slow but then increased dramatically. Oxalate was not biodegraded in any of the samples; this lack of degradation was also observed with selected bacterial strains that were isolated from cloud water (13).

Under UV light conditions (Light) with filtered cloud water, only the succinate concentrations did not evolve. Formaldehyde was continuously photoproduced, a result of the production of $^{\bullet}OH$ from H_2O_2 photolysis. Malonate was photoproduced up to a stationary concentration (60 h) (clouds 2 and 3). Oxalate was photodegraded up to a stationary state (60 h) that corresponded to the consumption-time of H_2O_2 in these samples (clouds 2 and 3). Formate was slowly degraded in cloud 3, up to 48 h, and was not degraded in cloud 2. The behavior of cloud 1 was somewhat different; a slow photoproduction of acetate and formate was observed, but oxalate was degraded continuously until the end of the experiment and was correlated with the presence of H_2O_2. The variations in the rates of organic compound phototransformation were related to the initial H_2O_2 concentrations in the three cloud waters (Tables 1 and 2). Consequently, the end of these transformations was linked to the total consumption of H_2O_2. In summary, from the observations that were made during incubations under UV light, the temporal evolutions of organic compound concentrations were highly variable, resulting from both the photoproduction and photodegradation processes. For cloud 1, the photodegradation rate was very low because the H_2O_2 concentration was 10–20 times lower than that in clouds 2 and 3, respectively.

In the presence of UV light and microorganisms (Microorganisms + Light case), we observed the sum of photochemical and microbial activities without synergy or inhibition. In clouds 2 and 3, the degradation rates of acetate, formate, and succinate, were similar with and without UV light because these compounds were not involved in any photochemical processes. For oxalate, the degradation rates were the same for light alone and light plus microorganisms; this observation is in agreement with the nonbiodegradability of this compound (clouds 2 and 3). Finally, for malonate, production and destruction are competitive (clouds 2 and 3). During the first part of the kinetic (up to 48 h), photoproduction dominated. Then, after 36 h, biodegradation began and became dominant. A similar behavior was noted for the degradation of acetate in cloud 1. The first photoproduction occurred before 72 h, and biodegradation then took over the relay. Formaldehyde was photoproduced and biodegraded. The apparent nontransformation of formaldehyde in the cloud waters in the presence of UV light and microorganisms (especially for clouds 2 and 3) revealed the competition between these two processes.

For all experiments, the organic compound biotransformation rates were similar between incubation under UV light or in darkness, and we did not observe an inhibition effect of reactive oxygen species over the microbial carbon metabolism.

Estimation of the Global Consequences of Microorganisms in Carbon Flux in the Atmosphere. From the number of cells (Table 1) and the degradation rates that were measured in the unfiltered microcosms that were incubated in the dark (i.e., the biodegradation rates, converted into $gC\ h^{-1}\ cell^{-1}$) (Table 3 and Table S4), we inferred the consumption of dissolved organic carbon species by microorganisms in clouds at the global scale (Table S4). Assuming a total mass of clouds of 1.94×10^{17} g on earth (14), microorganisms would constitute between 13 and 60 million tons of DOC, originating from formate, acetate, oxalate, malonate, succinate, and formaldehyde each year, on a global scale (results are based on clouds 1 and 2, respectively, in which the extreme lower and upper levels of microbial activity were measured). This is a conservative estimate of the total dissolved organic carbon biodegradation in clouds because other carbon compounds not measured here were most likely also consumed by cells. If we assume a bacterial growth efficiency on those compounds of 0 (i.e., these carbon sources are not used by microorganisms for producing biomass but are completely respired into CO_2), which is close to reality at low carbon concentrations (15), then the microbial respiration would lead to a global release of 51–215 million tons of CO_2 per year.

1. Kruisz C, Berner A, Brantner B (1993) A cloud water sampler for high wind speeds. *Proceedings of the EUROTRAC Symposium 1992*, eds Borrell PM, Borrell P, Cvitas T, Seiler W (SPB Academic, The Hague), pp 523–525.
2. Brantner B, Fierlinger H, Puxbaum H, Berner A (1994) Cloudwater chemistry in the subcooled droplet regime at Mount Sonnblick (3106 M A.S.L., Salzburg, Austria). *Water, Air, and Soil Pollution* 74(3):363–384.
3. Marinoni A, Laj P, Sellegri K, Mailhot G (2004) Cloud chemistry at the Puy de Dôme: Variability and relationships with environmental factors. *Atmos Chem Phys* 4(3): 715–728.
4. Parazols M, et al. (2007) Speciation and role of iron in cloud droplets at the puy de Dôme station. *J Atmos Chem* 57(3):299–300.
5. Stookey LL (1970) Ferrozine—A new spectrophotometric reagent for iron. *Anal Chem* 42(7):779–781.
6. Jaffrezo JL, Calas N, Bouchet M (1998) Carboxylic acids measurements with ionic chromatography. *Atmos Environ* 32(14–15):2705–2708.
7. Li Q, Sritharathikhun P, Motomizu S (2007) Development of novel reagent for Hantzsch reaction for the determination of formaldehyde by spectrophotometry and fluorometry. *Anal Sci* 23(4):413–417.
8. Lazrus AL, Kok GL, Gitlin SN, Lind JA, McLaren SE (1985) Automated fluorimetric method for hydrogen peroxide in atmospheric precipitation. *Anal Chem* 57(4):917–922.
9. Amato P, et al. (2005) Microbial population in cloud water at the Puy de Dôme: Implications for the chemistry of clouds. *Atmos Environ* 39(22):4143–4153.
10. Koutny M, et al. (2006) Acquired biodegradability of polyethylenes containing pro-oxidant additives. *Polym Degrad Stabil* 91(7):1495–1503.
11. Lundin A, Hasenson M, Persson J, Pousette A (1986) Estimation of biomass in growing cell lines by adenosine triphosphate assay. *Methods Enzymol* 133:27–42.
12. Stanley PE, Williams SG (1969) Use of the liquid scintillation spectrometer for determining adenosine triphosphate by the luciferase enzyme. *Anal Biochem* 29(3): 381–392.
13. Vaïtilingom M, et al. (2011) Atmospheric chemistry of carboxylic acids: Microbial implication versus photochemistry. *Atmos Chem Phys* 11(16):8721–8733.
14. Pruppacher HR, Jaenicke R (1995) The processing of water vapor and aerosols by atmospheric clouds, a global estimate. *Atmos Res* 38(1–4):283–295.
15. Eiler A, Langenheder S, Bertilsson S, Tranvik LJ (2003) Heterotrophic bacterial growth efficiency and community structure at different natural organic carbon concentrations. *Appl Environ Microbiol* 69(7):3701–3709.

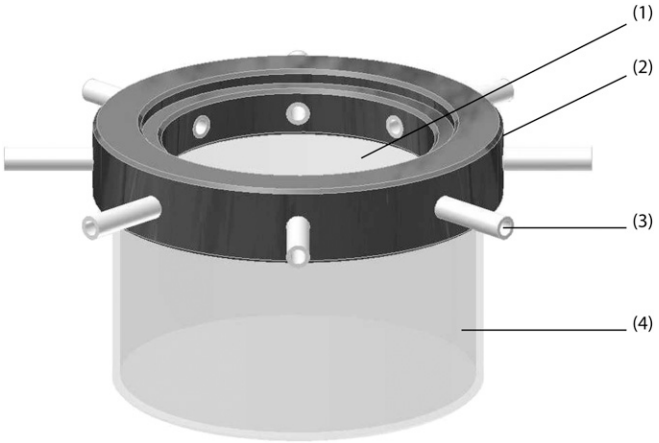

Fig. S1. Photo-bioreactor used for cloud water incubation under UV light . 1, Pyrex filter; 2, nylon lid; 3, Teflon tube of 8 mm Ø plugged with sterile cotton (eight vents); 4, cylindrical Pyrex crystallizer.

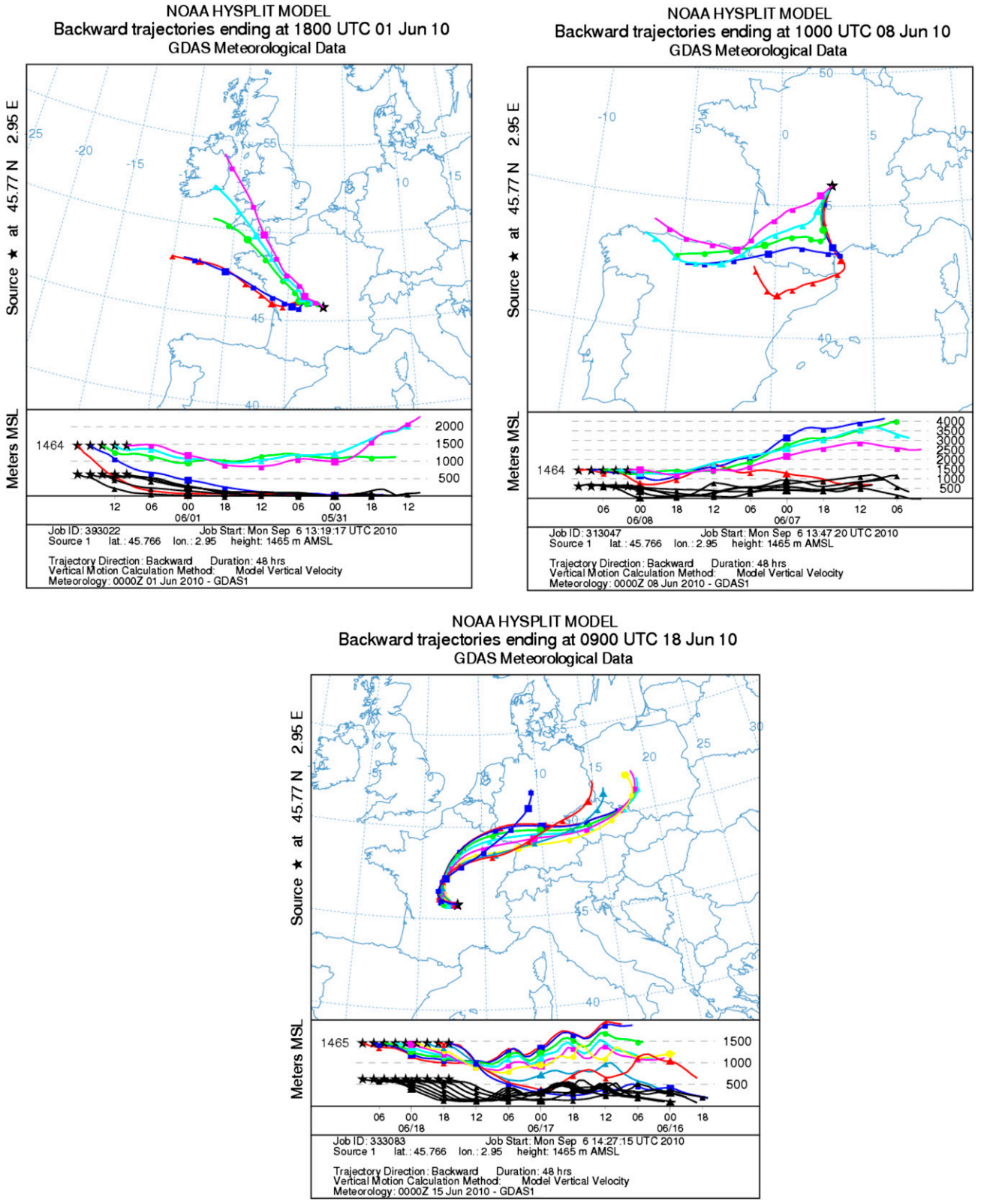

Fig. S2. The 48-h backward trajectories from the National Oceanic and Atmospheric Administration Hysplit model of clouds 1, 2, and 3.

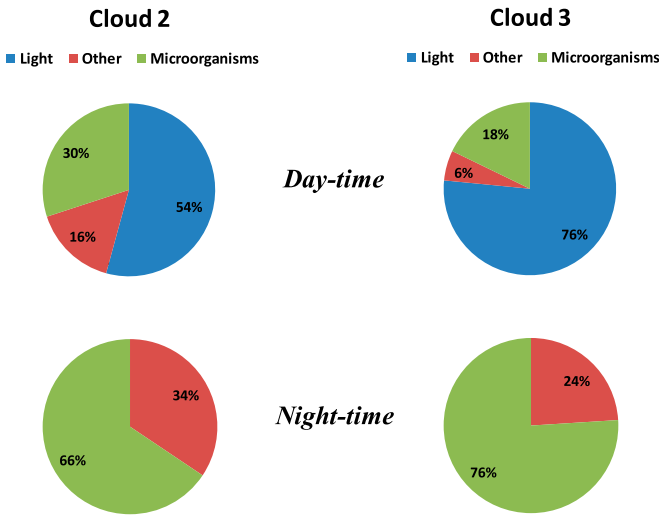

Fig. S3. Relative contribution of biotic and abiotic processes to H_2O_2 degradation during the incubation of clouds 2 and 3. "Light" (in blue) corresponds to pure photochemical processes; "Other" (in red) corresponds to nonphotochemically induced radical processes; and "Microorganisms" (in green) corresponds to a pure biodegradation processes. Percentages were calculated from the initial rates of degradation that were reported in Table S2.

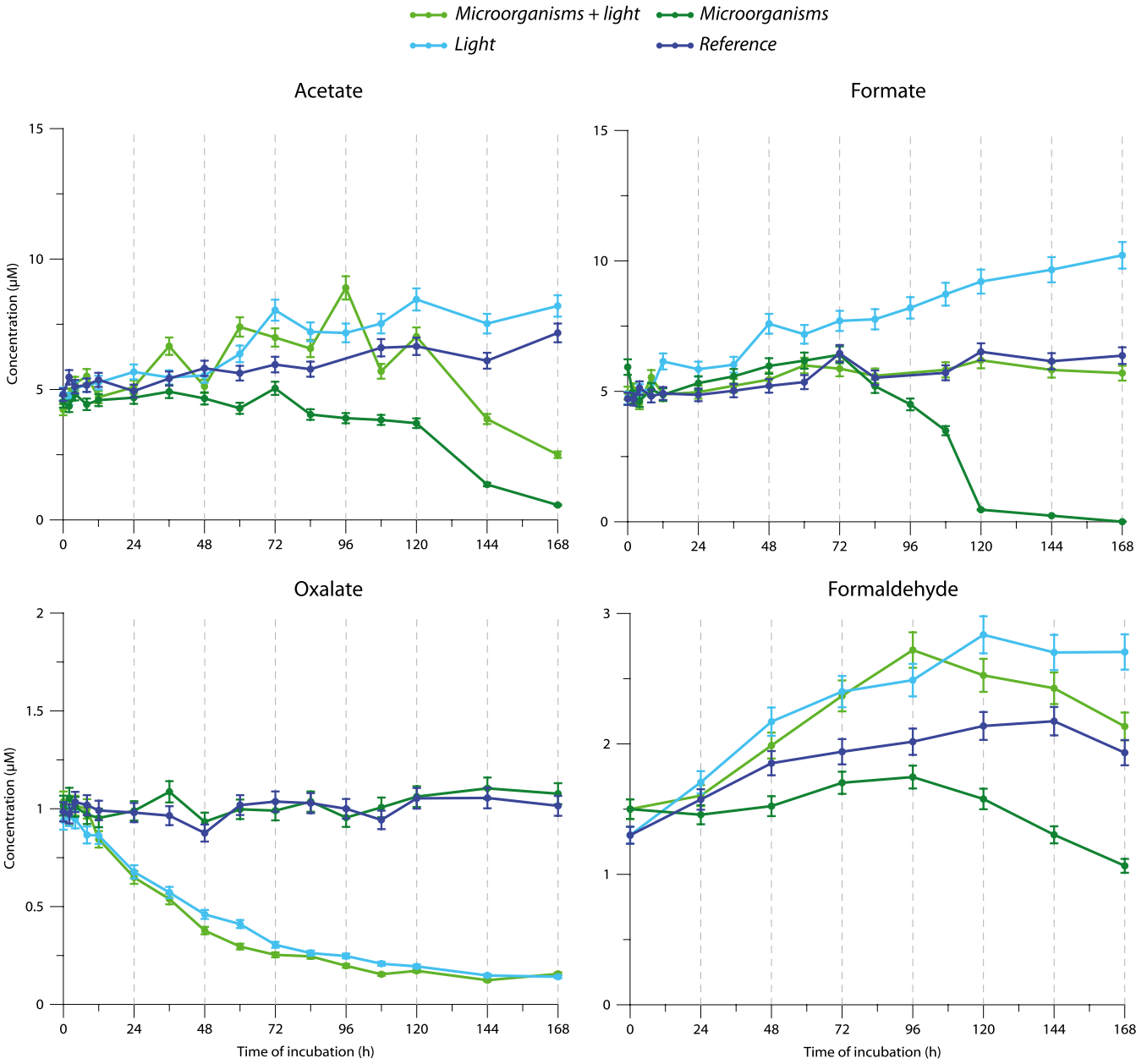

Fig. S4. Temporal evolution of carboxylic acids and formaldehyde concentrations during the incubation of cloud 1. The cloud 1 water sample was incubated at 17 °C under four incubation regimes for 7 d: unfiltered and in the presence or absence of UV radiation (Microorganisms + Light and Microorganisms, respectively), filtered and in the presence or absence of UV radiation (Light and Reference, respectively). Error bars represent the SEs of the chemical analysis (5%).

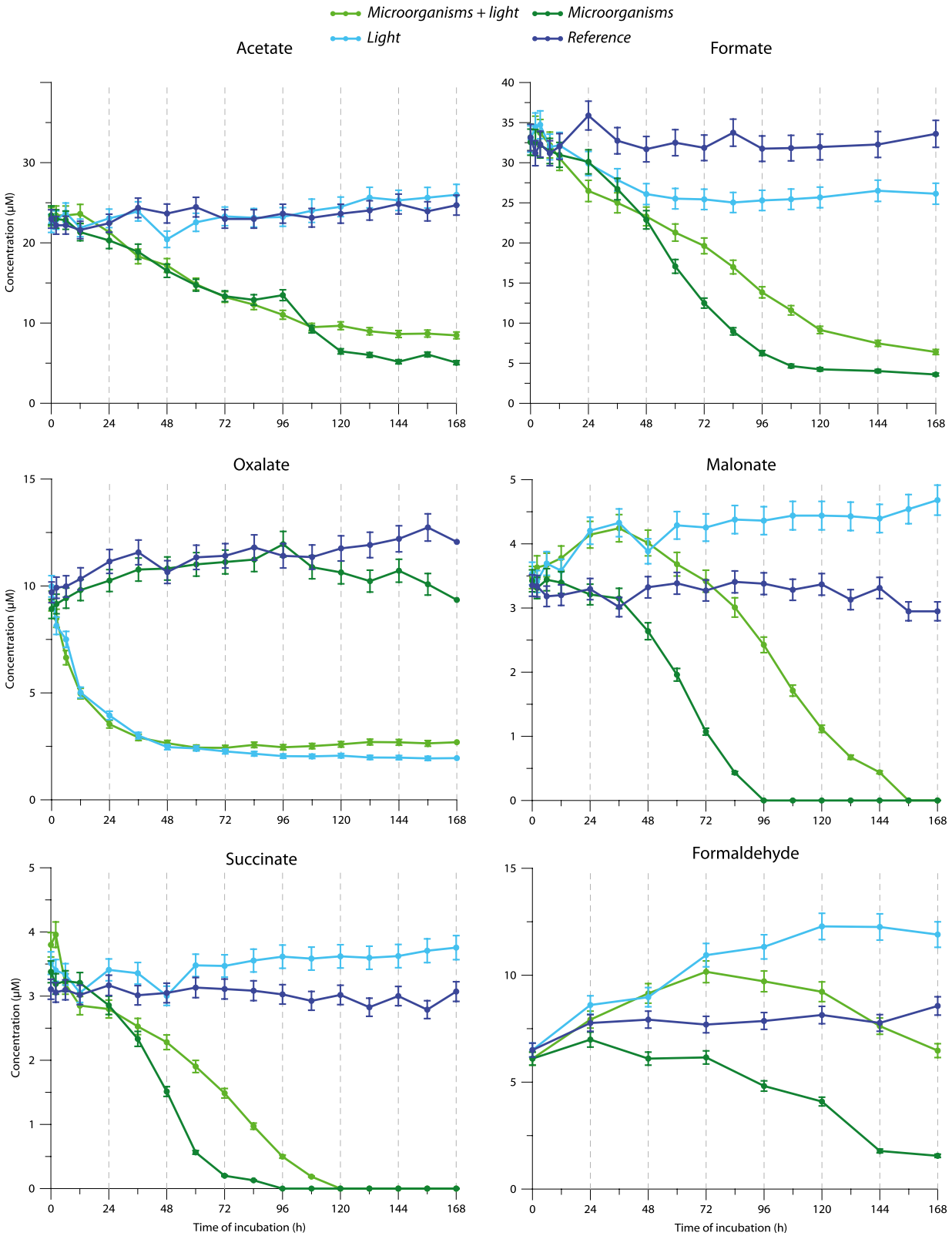

Fig. S5. Temporal evolution of carboxylic acids and formaldehyde concentrations during the incubation of cloud 3. The cloud 3 water sample was incubated at 17 °C under four incubation regimes for 7 d: unfiltered and in the presence or absence of UV radiation (Microorganisms + Light and Microorganisms, respectively), filtered and in the presence or absence of UV radiation (Light and Reference, respectively). Error bars represent the SEs of the chemical analysis (5%).

Table S1. Bio-physico-chemical measurements in cloud water samples

Measurements	Immediately after sampling	During incubation time			
		Start	Every 12 h	Every 24 h	End
PH	■	■		■	■
Conductivity	■	■			■
TOC	■	■			■
Ionic chromatography	■	■	■	■	■
Fe(II)/Fe(III) assay	■	■			■
H_2O_2 concentration	■	■	■	■	■
Formaldehyde assay	■	■	■	■	■
ATP/ADP*	■	■	■	■	■
Total cells counts	■	■			■
Cultivable cells counts		■			■

After 2 and 6 h of incubation, ionic chromatography analyses and H_2O_2 assays were performed for each sample.
*Only performed at the beginning and end of the incubation for the filtered (sterilized) samples to assess the sterility.

Table S2. Calculated values of the initial transformation rates of H_2O_2, linked to biotic and abiotic processes occurring during the incubation of clouds 1, 2, and 3

Process	Cloud 1	Cloud 2	Cloud 3
	Initial rate of H_2O_2 transformation ($\times 10^{-11}$ M·s^{-1})		
Abiotic			
Light	−0.9	−33.8	−97.9
Other	0	−9.8	−7.2
Biotic			
Microorganisms	0	−18.7	−22.8

"Light" corresponds to pure photochemical processes, "other" corresponds to nonphotochemically induced radical processes, and "microorganisms" corresponds to pure biodegradation processes. Negative values indicate the disappearance of H_2O_2 from the medium.

Table S3. Initial transformation rates of carboxylic acids and formaldehyde in the presence and absence of UV light and/or microorganisms during the incubation of cloud 2

Event no.	Parameters	Acetate	Formate	Succinate	Oxalate	Malonate	Formaldehyde
		Rate of transformation ($\times 10^{-11}$ M·s^{-1})					
Cloud 1	Light	**0.5**	**0.7**	—	−0.4	—	0.2
	Microorganisms	−2.3 (72 h to end)	−13.9 (72 h to end)	—	0	—	−0.3 (60 h to end)
	Microorganisms + Light	0.7 (0 h to 84 h)	0	—	−0.4	—	0.3 (0 h to 96 h)
		−0.9 (84 h to end)					−0.2 (96 h to end)
Cloud 2	Light	0	0	0	−4.0 (0 h to 60 h)	**0.3** (0 h to 60 h)	0.2
	Microorganisms	−15.5	−17.5 (48 h to end)	−4.5	0	−4.2 (36 h to end)	−0.3
	Microorganisms + Light	−15.6	−16.1 (48 h to end)	−3.5	−2.7 (0 h to 60 h)	−4.3 (36 h to end)	0
Cloud 3	Light	0	−2.6 (0 h to 48 h)	0	−8.5 (0 h to 48 h)	**0.5** (0 h to 48 h)	0.9
	Microorganisms	−5.8	−12.5	−3.4	0	−3.5 (36 h to end)	−1.0
	Microorganisms + Light	−4.4	−8.5	−2	−8.0 (0-48 h)	0.6 (0 h to 36 h)	0
						−2.4 (36 h to end)	

A negative value indicates the disappearance of the organic compounds from the medium. Values in bold represent production of the study compounds. In the case where a noncontinuous transformation occurred, the time period used for the linear regression is indicated in parenthesis. A dash indicates no transformations observed for the "Reference" sample (i.e., sterilized sample incubated in darkness).

Table S4. Estimates of the amount of CO_2 released by microbial respiration in clouds

Observed and inferred	Cloud 1	Cloud 2	Cloud 3
Observed in natural clouds			
Cell concentration (mL^{-1})	$3.0\ 10^{4}$	$8.0\ 10^{4}$	$9.0\ 10^{4}$
Carbon biodegradation rate (gC h^{-1} $cell^{-1}$)	$2.71\ 10^{-13}$	$4.29\ 10^{-13}$	$3.28\ 10^{-13}$
Inferred at global scale*			
Total number of cells in clouds	$5.82\ 10^{21}$	$1.55\ 10^{22}$	$1.75\ 10^{22}$
Carbon biodegradation rate (gC h^{-1})	$1.58\ 10^{9}$	$6.65\ 10^{9}$	$5.73\ 10^{9}$
Carbon biodegradation rate (tons of C yr^{-1})	$1.38\ 10^{7}$	$5.83\ 10^{7}$	$5.03\ 10^{7}$
Amount of CO_2 released by microbial respiration (tons yr^{-1})	$5.06\ 10^{7}$	$2.14\ 10^{8}$	$1.84\ 10^{7}$

The cell concentrations are listed in Table 1, and the degradation rates from Table 3 were converted into gC h^{-1} $cell^{-1}$. The total mass of clouds follows the conclusions of Pruppacher and Jaenicke (14).
*Total mass of clouds = 1.94×10^{17} g (14).